Wind and Structures, *Vol. 27, No. 2 (2018) 111-121*
DOI: https://doi.org/10.12989/was.2018.27.2.111

Effects of aspect ratio on laboratory simulation of tornado-like vortices

Zhuo Tang[1], Delong Zuo[*1,2], Darryl James[3], Yuzuru Eguchi[4] and Yasuo Hattori[4]

[1]*National Wind Institute, Texas Tech University, Lubbock, TX 79409, USA*
[2]*Department of Civil, Environmental and Construction Engineering, Texas Tech University, Lubbock, TX 79409, USA*
[3]*Department of Mechanical Engineering, Texas Tech University, Lubbock, TX 79409, USA*
[4]*Fluid Dynamics Sector, Civil Engineering Research Laboratory, Central Research Institute of Electric Power Industry, Abiko 1646, Abiko-shi, Chiba-ken, 270-1194 Japan*

(Received April 12, 2018, Revised June 27, 2018, Accepted July 9, 2018)

Abstract. Experiments were conducted in a large-scale Ward-type tornado simulator to study tornado-like vortices. Both flow velocities and the pressures at the surface beneath the vortices were measured. An interpretation of these measurements enabled an assessment of the mean flow field as well as the mean and fluctuating characteristics of the surface pressure deficit, which is a manifestation of the flow fluctuation aloft. An emphasis was placed on the effect of the aspect ratio of the tornado simulator on the characteristics of the simulated flow and the corresponding surface pressure deficit, especially the evolution of these characteristics due to the transition of the flow from a single-celled vortex to a two-celled vortex with increasing swirl ratio.

Keywords: tornado-like vortex; surface pressure deficit; aspect ratio; swirl ratio

1. Introduction

Tornadoes are a type of non-synoptic wind storm. They differ from synoptic winds in that they are localized swirling flows instead of straight-line flows or flows that can be treated as locally traveling along a straight line, such as in the case of hurricanes. Due to the well-recognized devastating effects of tornadoes on the built environment, many investigations have been conducted to study the structure of tornadic flow and the loading on structures by tornadoes.

The study of tornadic flows, in particular, can be classified into three approaches, all of which have both strengths and weaknesses. The first approach utilizes either direct measurements of tornado winds, primarily using Doppler radars (e.g., Karstens, *et al*. 2010, Wurman and Gill 2000, Wurman *et al*. 2013), or indirect estimation of tornado wind speeds based on surveys of damages caused by the storms (e.g., Fujita 1971, Mehta *et al*. 1976, Yang *et al.* 2018). While this type of study has produced much knowledge of historic significance regarding tornadoes, they still face a number of challenges. Due to the inadequate understanding of tornado genesis and the destructive nature of tornadic winds, direct measurements often require significant efforts and are limited by many practical difficulties. Also, measurements by radars to date still lack the necessary resolution required for revealing the characteristics of the flow near the ground which are relevant to the assessment of tornadic loading on structures. In addition, while post-disaster surveys have historically served a significant role in qualitative or semi-quantitative understanding of tornadic winds and their effects on structures, the inferences from the surveys have mostly been derived based on the knowledge of wind loading by boundary-layer-type winds, and the uncertainties that are inherently embedded in these inferences can be difficult to track.

The second approach relies on numerical modeling based on computational fluid dynamics (CFD) to simulate model-scale tornado-like vortices in a tornado chamber (e.g., Bryan, *et al.* 2017, Ishihara *et al.* 2011, Lewellen *et al.* 1997, Nasir 2017, Natarajan and Hangan 2012, Nolan and Farrell 1999, Nolan *et al*. 2017) This numerical approach has seen many significant advancements, especially in recent years. However, challenges in numerical modeling of turbulent flows, with tornado-like flows being particularly complex, largely due to the uncertainty of the near wall modeling and inlet conditions, still remain. For example, many of the previous studies of tornado-like flows that used large eddy simulation (LES) employed the law-of-the-wall for the velocity of the first grid point off the wall. This may be applicable in regions far from the core radius, but is questionable near and within the core where significant vertical pressure gradients exist. To mitigate this problem, more recent LES studies of tornado-like flows have used the dynamic Smagorinsky-Lilly subgrid turbulence model in the near-wall region (typical y^+ values of order 1) to dissipate energy (e.g., Liu *et al.* 2018, Liu *et al*. 2018). Inlet conditions for LES models have also been shown to affect the flow simulations in a variety of flows (none tornado-like) as discussed in Tabor and Baba-Ahmadi (2010). Current techniques for the generation of inflow tuerbulence can be classified into one of three categories – the synthesis inlets, the precursor simulation and the recycling methods (Liu and Pletcher 2006). The precursor simulation and the recycling methods are computationally expensive

*Corresponding author, Associate Professor
E-mail: delong.zuo@ttu.edu

ISSN: 1226-6116 (Print), 1598-6225 (Online)

(Aboshosha *et al.* 2015), and it has been suggested that synthesis methods are inherently inaccurate and require the provision of an inlet development section during which the random fluctuations develop into true turbulence (Tabor and Baba-Ahmadi, 2010). Although a recent study has proposed a method that can be used to generate inflow boundary conditions that match the spectra and coherence of flows in the atmospheric boundary layer (Aboshosha *et al.* 2015), the applicability of this method in the generation of inflow conditions for tornadic flows remains to be clarified. Nonetheless, even with the aforementioned challenges numerical modeling of tornadic flows offers advantages such as its capability to model a large-enough domain for adequate study of tornadic loading on structures. With continued improvement, the numerical approach is expected to play an increasing role in the study of both the flow characteristics and the effects of tornadoes on the built environment.

The third approach uses tornado simulators to physically generate tornado-like vortices and to infer the characteristics of full-scale tornadoes based on observations from these physical simulations. Despite its limitations, such as its inability to generate vortices of adequate size to facilitate the studies of tornadic loading on some structures, this approach has gained much momentum because it allows studies of tornado-like flows in a controlled, repeatable manner and results from the experiments can be used to validate numerical simulations. More importantly, a number of studies have shown that the simulated flows can resemble full-scale tornadoes in many characteristics (e.g., Church *et al.* 1979, Haan *et al.* 2008, Refan and Hangan 2018, Tang *et al.* 2018). The study presented here is based on physical simulation of tornado-like vortices.

Systematic laboratory simulations of tornado-like winds started with the pioneering work by Ward (1972) more than 4 decades ago, and many tornado simulators have been built subsequently, mostly based on variations of Ward's design. The early experiments in Ward-type simulators (e.g., Church *et al.* 1979, Jischke and Parang 1974, Snow *et al.* 1980) have revealed many major characteristics of tornado-like flows and the dependence of these characteristics on the parameters that were theoretically identified to govern the dynamics and geometry of tornadic vortices (Lewellen 1962). It was observed that the swirl ratio critically influences the transition of the simulated tornadic flow from a single-celled to a two-celled vortex and eventually to multiple vortices. By contrast, the early experiments indicated that the radial Reynolds number and the aspect ratio have secondary effects on the simulations (Church *et al.* 1979, Davies-Jones 1973). In particular, it was suggested that the core radius of the simulated flows is insensitive to the radial Reynolds number as long as this number is sufficiently large. The importance of the swirl ratio on the simulation of tornado-like vortices has also been confirmed by experiments in simulators that are either not of the Ward-type, such as the closed-circuit-type tornado simulator at Iowa State University (Haan *et al.* 2008), or not strictly of the Ward-type, such as a scaled model of the WindEEE dome at the University of Western Ontario (Refan and Hangan 2016), which, when configured to generate stationary vortices, differs from the Ward-type simulators in that it does not have a bounded confluence region of constant height.

Despite the continued advancement in laboratory simulation of tornado-like vortices, most of the previous studies have focused on the mean characteristics of the simulated flow and those of the resultant surface pressure deficit. A recent study (Tang *et al.* 2018) was conducted to investigate both the mean and turbulent characteristics of flows simulated in a large-scale Ward-type simulator as well as the characteristics of both the mean and the fluctuating components of the surface pressure within simulated vortices. It was revealed that not only the mean structures but also the fluctuations of the flow and the surface pressure are dependent on the swirl ratio. In addition, it was found that the mean and fluctuation characteristics of the flow are independent of large radial Reynolds number. This paper presents the outcomes of a follow-up study that further investigate the effects of the aspect ratio on laboratory simulation of tornado-like vortices.

2. Experimental configuration

The experiments conducted in this study is an extension of those reported in Tang *et al.* (2018). Therefore, the configurations of the experiments are also similar to those used in that previous study. For completeness, the essence of the experimental configurations is summarized herein. The facility used in the experiments is a large-scale Ward-type simulator at Texas Tech University known as VorTECH, which is schematically shown in Fig. 1. This apparatus has a cylindrical testing chamber of 10.2 m in diameter, an octagon updraft hole of 4 m in diameter, 64 turning vanes in the form of symmetric airfoils at the periphery of the chamber and a honeycomb that serves as the baffle in Ward-type simulators. The updraft is provided by 8 fans at the top, the speed of which can be varied to control the flow rate; while the diameter of the updraft hole is fixed, the heights of the chamber and the turning vanes can be adjusted between 1 m and 2 m to control the internal aspect ratio of the apparatus.

The experiments utilized a Cobra probe (Turbulent Flow Instrumentation Pty Ltd) and a 12-hole Omniprobe (Aeroprobe Corporation) for the measurement of flow velocity. The two probes are chosen for their complementing capabilities. The Cobra probe is capable of measuring turbulence at frequencies in excess of 2000 Hz, but it can only measure flows within a ±45° cone. By contrast, while the Omniprobe is not capable of accurately measuring high-frequency turbulence, it can measure the mean velocity of the flow approaching from ±150° relative to its axis. The Cobra probe was used whenever at least 98% of the flow was reported by the manufacturer-supplied software to be valid; otherwise the Omniprobe was used. All the velocity measurements were carried out within a vertical plane through the vertical axis of the simulator. Fig. 2 shows the velocity measurement grid for one experimental configuration (z being the height above the floor, r being the radial distance from the vertical axis of the

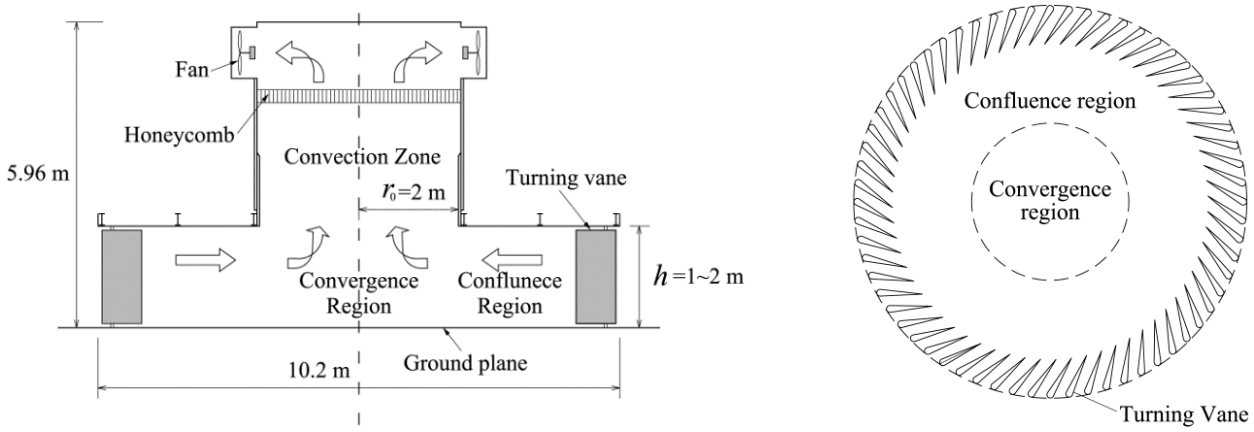

Fig. 1 A schematic illustration of VorTECH

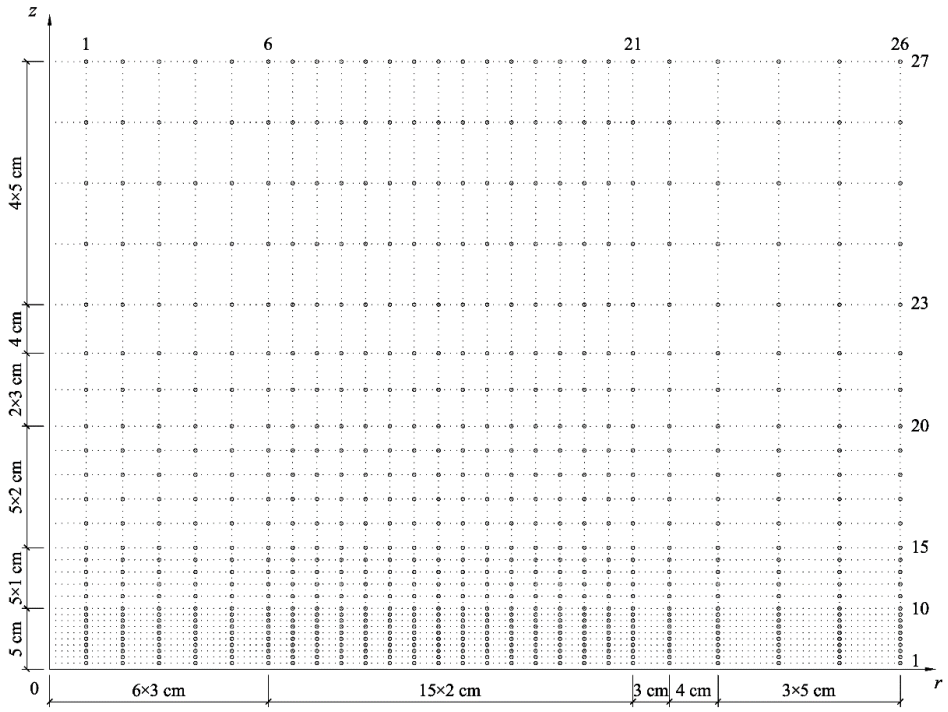

Fig. 2 An example of the flow velocity measurement grid

simulator). The density of the measurement points in the vertical direction was higher at heights immediately above the floor because a major objective of the study is to facilitate future studies of tornado loading on structures near the surface of the earth. The density of the measurement points in the horizontal direction was the highest in the region between radial distances of 18 cm and 48 cm. This was because the mean tangential velocities of the largest values were measured within this region. For the other experimental configurations, the placement of the probes in the vertical direction was the same as that shown in Fig. 2, but the number and separations of the measurement points in the horizontal direction were varied to enable dense measurements in areas of large mean tangential velocities.

At each measurement point, a two-minute record was collected by either the Cobra probe or the Omniprobe. The sampling frequency of the Cobra probe was 625 Hz; that of the Omniprobe was 300 Hz.

In addition to the velocity measurements, a Scanivalve system with an uncertainty of ± 1.2 Pa was used in the experiments to measure the surface pressures at 195 axisymmetric taps evenly spaced at 0.019 m along a radial line on the floor of the simulator. For every experimental configuration, 10 two-minute surface pressure measurements were conducted at a sampling frequency of 300 Hz. In the following, the statistics of the surface pressure are based on the ensemble of 10 measurements, while those of the flow velocity are based on single two-minute measurements only.

3. Estimation of controlling parameters

Although it has long been established that the dynamics of tornado-like vortices is controlled by the swirl ratio and the radial Reynolds number and that the geometry of such vortices are governed by the aspect ratio (Lewellen 1962, Davies-Jones 1973), the manner in which the swirl ratio and the radial Reynolds number are defined and estimated has varied in previous literature. In this study, the definitions of the three controlling parameters follow those presented in Church *et al.* (1979), that is

$$S = r_0\Gamma / (2Qh) \tag{1}$$

$$Re_r = Q / (2\pi\nu) \tag{2}$$

$$a = h / r_0 \tag{3}$$

where S, Re_r and a are the swirl ratio, the radial Reynolds number and the aspect ratio, respectively, h and r_0 are the depth and radius of the convergence region, which are taken as the height of the turning vanes and the radius of the updraft hole (as shown in Fig. 1), respectively, Q is the volume flow rate per unit axial length, Γ is the circulation, and ν is the kinematic viscosity of air. The estimation of the volume flow rate per unit axial length and the circulation follows the approach used in Tang *et al.* (2018)

$$Q = \frac{2\pi r_0}{h}\sum_{n=1}^{N}\left(\bar{V}_{r,n}\times\Delta h_n\right) \tag{4}$$

$$\Gamma = \frac{2\pi r_0}{h}\sum_{n=1}^{N}\left(\bar{V}_{\theta,n}\times\Delta h_n\right) \tag{5}$$

where $\bar{V}_{r,n}$ and $\bar{V}_{\theta,n}$ are the mean radial and tangential velocities of the flow at the n^{th} point of measurement along a vertical line originated from the edge of the updraft hole, Δh_n is half the distance between the two measurement points surrounding this point, and N is the total number of measurement points. Δh_n ranges between 0.5 cm over the heights near the simulator floor to 10 cm over the upper heights. This approach apparently assumes that the flow beneath the periphery of the updraft hole is representative of the inflow that results in the tornado like vortex. It is consistent with the manner in which the circulation is calculated in Church *et al.* (1979), because the locations at the radius of the updraft hole can be considered to be in the far-field of the simulated vortices.

In the experiments, the aspect ratio of the simulator was fixed at 0.5, and the swirl ratio was varied by adjusting the orientations of the turning vanes. In the following, the observed characteristics of the flow and the surface pressure from these experiments are compared with the corresponding ones observed in previously reported simulations (Tang *et al.* 2018) at similar swirl ratios but a different aspect ratio of unity to investigate the effect of the aspect ratio on laboratory tornado simulations. It is worth noting that since the objective of the study was to investigate the effects of the aspect ratio on the flow and surface pressure fields, the orientations of the turning vanes were purposely adjusted in the new experiments so that the swirl ratios are close to the corresponding values achieved in the previous study, rather than orienting the turning vanes at the angles used in the previous study to investigate the effects of the aspect ratio on the swirl ratio. Because all the simulations were conducted at radial Reynolds numbers that are larger than 3.11×10^5, the effects of this parameter on both the mean (e.g., Church *et al.* 1979, Refan and Hangan 2016) and turbulent (Tang *et al.* 2018) characteristics of the flow are inconsequential.

4. Effects of the aspect ratio on the flow chracteristics

Fig. 3 shows the mean flow fields of four representative vortices generated in VorTECH, two at an aspect ratio of unity, which has been presented in Tang *et al.* (2018), and the other at an aspect ratio of 0.5 resulting from the new experiments. The arrows in the graphs represent the resultant of the mean radial ($\bar{V}_r$) and axial (i.e., vertical $\bar{V}_z$) components of the velocity, and the background color represents the mean tangential component ($\bar{V}_\theta$) of the velocity. The mean radial and axial velocities shown in the graphs are directly from the measurements, while the mean tangential velocities are results from linear interpolations of the measured mean tangential velocities. The effects of the swirl ratio are clearly reflected by the evolution of the mean flow fields at both aspect ratios. At each aspect ratio, the core of the simulated vortex, represented by the region surrounded by the radial location of the maximum mean tangential velocity at each height, is larger at the larger swirl ratio. More importantly, for both aspect ratios, the two vortices at the smaller swirl ratios ($S = 0.17$ for $a = 1$ and $S = 0.24$ for $a = 0.5$) both have a single cell and the vortices at the higher swirl ratios ($S = 0.84$ for $a = 1$ and $S = 0.78$ for $a = 0.5$) both have two cells, the presence of which are signified by the apparent downdraft in the center of these vortices. Such transition of the flow from a single-celled vortex to a two-celled vortex with increasing swirl ratio has been well documented in many previous studies. Fig. 3 also shows an effect of the aspect ratio on the simulated vortices. For the single-celled vortices simulated at similar swirl ratios, the one simulated at the smaller aspect ratio has a smaller core, and the same observation can be made for the two two-celled vortices. This is clear evidence of the effect of the aspect ratio on the geometry of simulated vortices.

The effects of the aspect ratio on the geometry of the vortex can be observed more clearly in Fig. 4 , which shows the vertical profile of the local core radius, r_{cz}, defined as the distance between the point where the maximum mean tangential velocity at height z ($\bar{V}_{\theta z\max}$) occurs and the

simulator axis, for the four vortices. It is seen that for simulations at similar swirl ratios, smaller aspect ratio results in a smaller local core radius at almost every height for the single-celled vortices and at every height for the two-celled vortices.

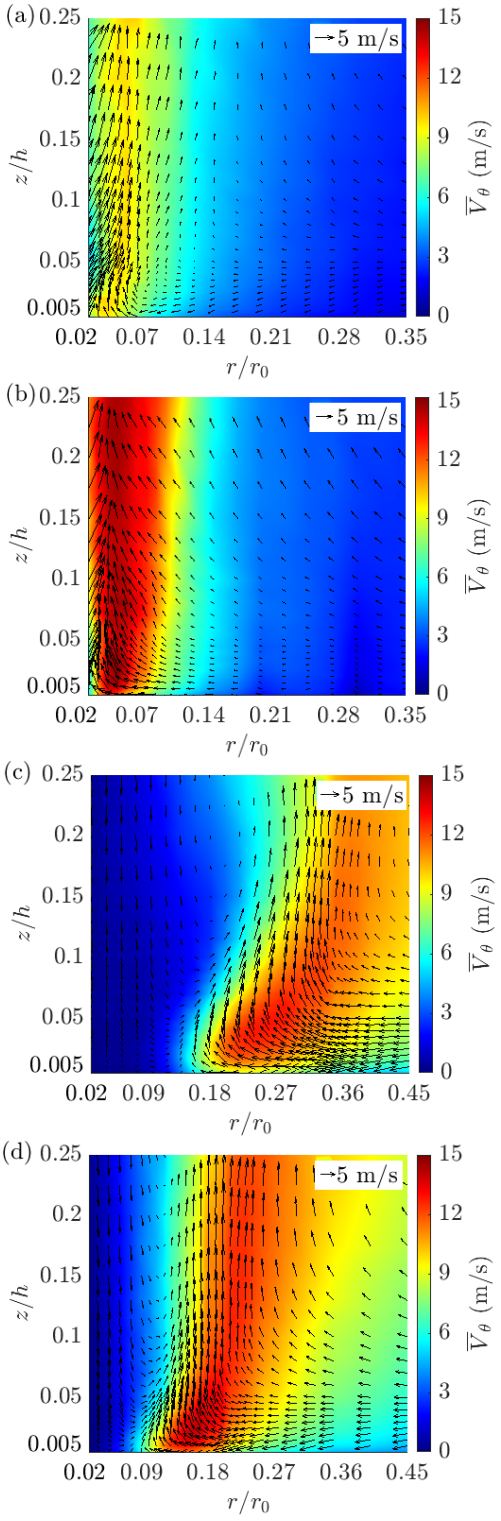

Fig. 3 Mean flow fields at aspect ratios and swirl ratios of (a) S=0.17, a=1.0, (b) S=0.24, a=0.5, (c) S=0.84, a=1.0 and (d) S=0.78, a=0.5

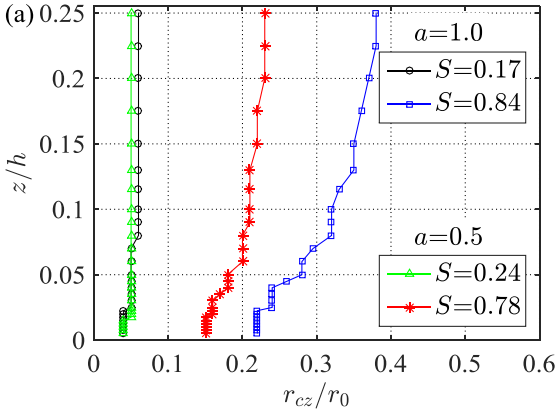

Fig. 4 Vertical profiles of the local core radius of simulated vortices

Fig. 5 shows the radial profiles of the normalized (by the maximum mean tangential velocity at the height of interest, $\overline{V}_{\theta z\max}$) mean tangential velocity of the four simulated vortices at the height of the overall maximum tangential velocity, z_c, and the corresponding profiles at two heights below and two heights above z_c. Also included in this figure are the corresponding profiles according to the Burgers-Rott vortex model (Burgers 1948, Rott 1958) for the single-celled vortices and the Sullivan vortex model (Sullivan, 1959) for the two-celled vortices represented by Eqs. (6) and (7), respectively

$$\overline{V}_\theta = 1.4\overline{V}_{\theta z\max}\left(r/r_{cz}\right)^{-1}\left\{1-\exp\left[-1.2564\left(r/r_{cz}\right)^2\right]\right\} \quad (6)$$

$$\overline{V}_\theta = \overline{V}_{\theta z\max}\left(r/r_{cz}\right)^{2.4}\left[0.3+0.7\left(r/r_{cz}\right)^{7.89}\right]^{-0.435} \quad (7)$$

as well as the radial profile of the mean tangential velocity prescribed by the Rankine combined vortex model with a decay constant of 1.0 and the modified Rankine combined vortex model with a decay constant of 0.7 (Wurman *et al.* 2007). The original and modified Rankine combined vortex models state that

$$V_\theta = \begin{cases} \left(\dfrac{r}{r_{cz}}\right)V_{\theta z\max} & r \le r_{cz} \\ \left(\dfrac{r_{cz}}{r}\right)^{\alpha} V_{\theta z\max} & r > r_{cz} \end{cases} \quad (8)$$

where α is the decay constant.

Figs. 5(a) and 5(c) for the case of unit aspect ratio have been presented in Tang *et al.* (2018). It has been concluded in that study based on graphs such as these that the radial profile of the normalized mean tangential velocity follows that of the Burgers-Rott and Sullivan models, depending on whether the vortex is single-celled or two-celled. It was also concluded that the experimental data does not agree well with the modified Rankine combined vortex model. Fig. 5

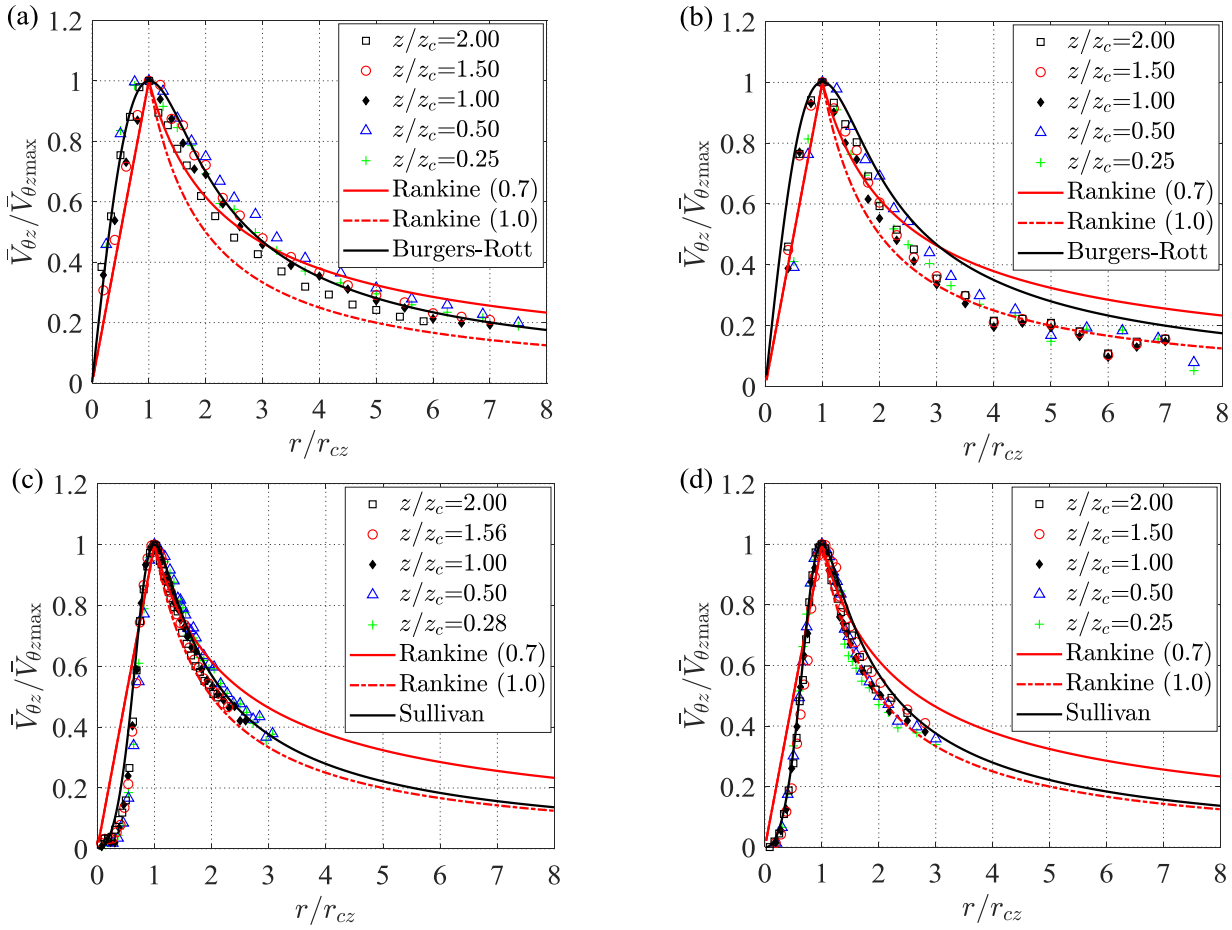

Fig. 5 Radial profiles of mean tangential velocity of vortices simulated at (a) S=0.17, a=1.0, (b) S=0.24, a=0.5, (c) S=0.84, a=1.0 and (d) S=0.78, a=0.5

shows that these conclusions are also valid for the simulations at an aspect ratio of 0.5 and that the radial profiles of the mean tangential velocity also deviate from the Rankine combined vortex model with a decay constant of 1.0 regardless of the aspect ratio. This further suggests that the aspect ratio does not significantly affect the structure of the mean tangential velocity field, although it affects the size of the vortex.

Although the Burgers-Rott and Sullivan models can closely fit the radial profile of the normalized mean tangential velocities, their performances in fitting the profiles of the other mean flow components are not as satisfactory, regardless of the swirl ratio and aspect ratio. Figs. 6 and 7 show the radial profiles of the normalized mean radial velocity ($\bar{V}_{rz}/\bar{V}_{rz\max}$, $\bar{V}_{rz}$ being the mean radial velocity at height z and $\bar{V}_{rz\max}$ being the maximum mean radial velocity at height z) and the axial profiles of the normalized mean axial velocity ($\bar{V}_{zr}/\bar{V}_{zr\max}$ when $\bar{V}_{zr}$ is positive at all heights, $\bar{V}_{zr}$ being the mean axial velocity at height z at the radial position of interest, and $\bar{V}_{zr\max}$ being the maximum axial velocity along the height at the radial position of interest, or $\bar{V}_{zr}/|\bar{V}_{zr}|_{\max}$, when $\bar{V}_{zr}$ is negative at all heights), respectively, of the four simulated vortices. In Fig. 6, the radial position is normalized by the radial position at which the maximum mean radial velocity occurs ($r_{\bar{V}_{rz\max}}$); in Fig. 7, the axial position (i.e., height) is normalized by the height at which the maximum positive mean axial velocity or the maximum of the absolute value of the negative mean axial velocity occurs ($z_{\bar{V}_{zr\max}}$ or $z_{|\bar{V}_{zr}|_{\max}}$). Also included in Fig. 6 are the radial profiles of the mean radial velocity of the single-celled vortices at the height of the overall maximum tangential velocity as prescribed by the Burgers model

$$\bar{V}_r = Ar \tag{9}$$

and the corresponding profiles of the two-celled vortices as prescribed by the Sullivan model

$$\bar{V}_r = Ar - \frac{6\nu}{r}\left(1 - e^{-\frac{Ar^2}{2\nu}}\right) \tag{10}$$

where $A = 12.476\nu_t / r_C^2$, in which ν_t is the turbulent viscosity, estimated based on Cobra probe measurements.

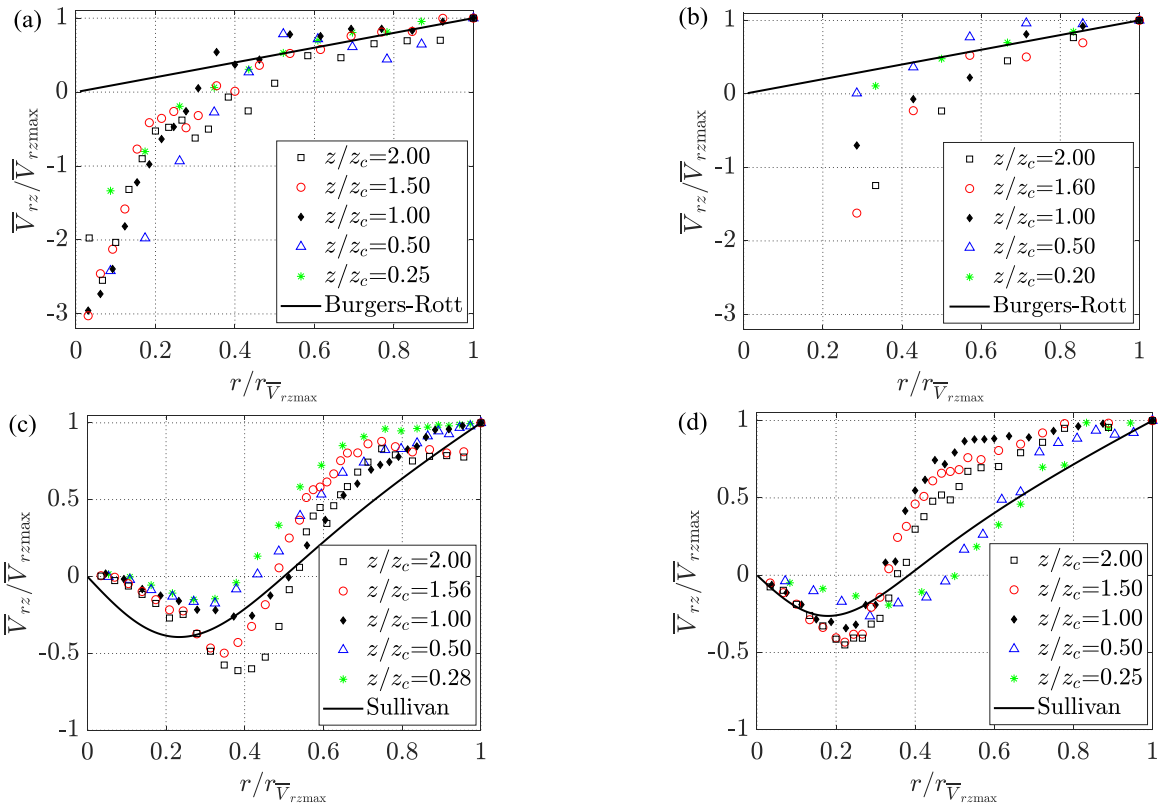

Fig. 6 Radial profiles of mean radial velocity of vortices simulated at (a) S=0.17, a=1.0, (b) S=0.24, a=0.5, (c) S=0.84, a=1.0 and (d) S=0.78, a=0.5

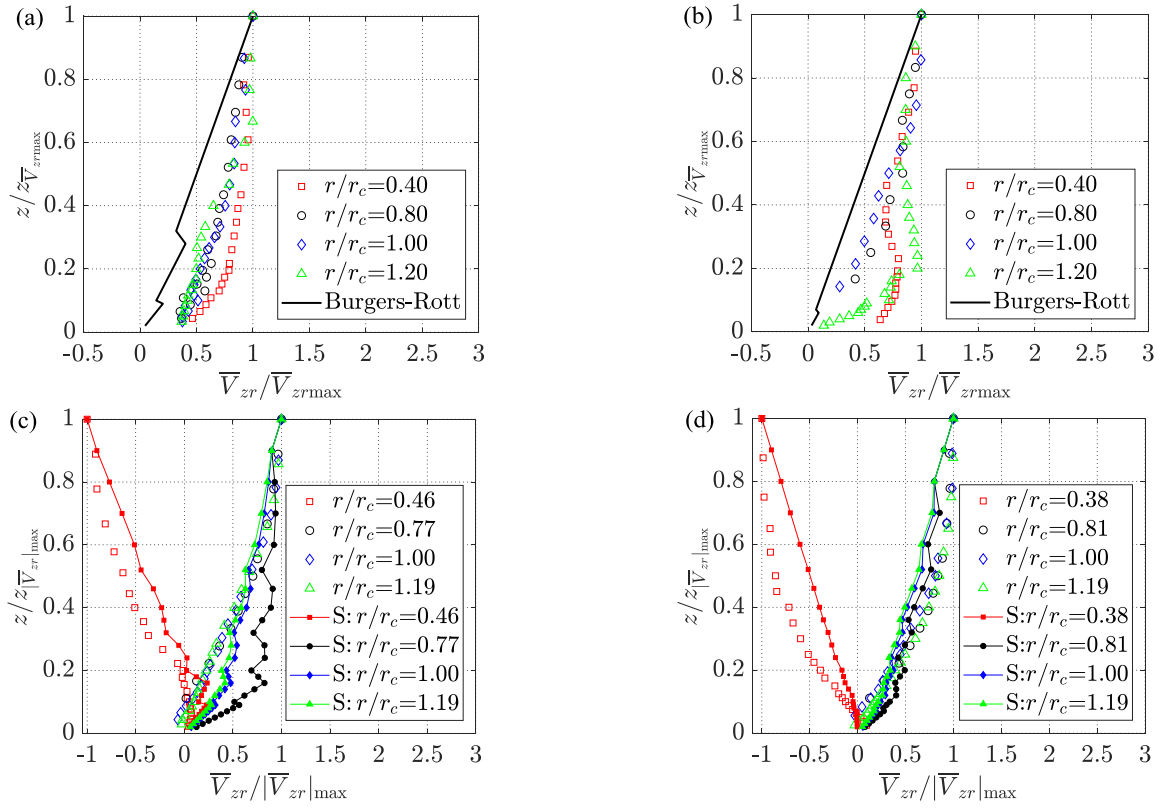

Fig. 7 Axial profiles of mean axial velocity of single-celled vortices simulated at (a) S=0.17, a=1.0, (b) S=0.24, a=0.5, (c) S=0.84, a=1.0 and (d) S=0.78, a=0.5

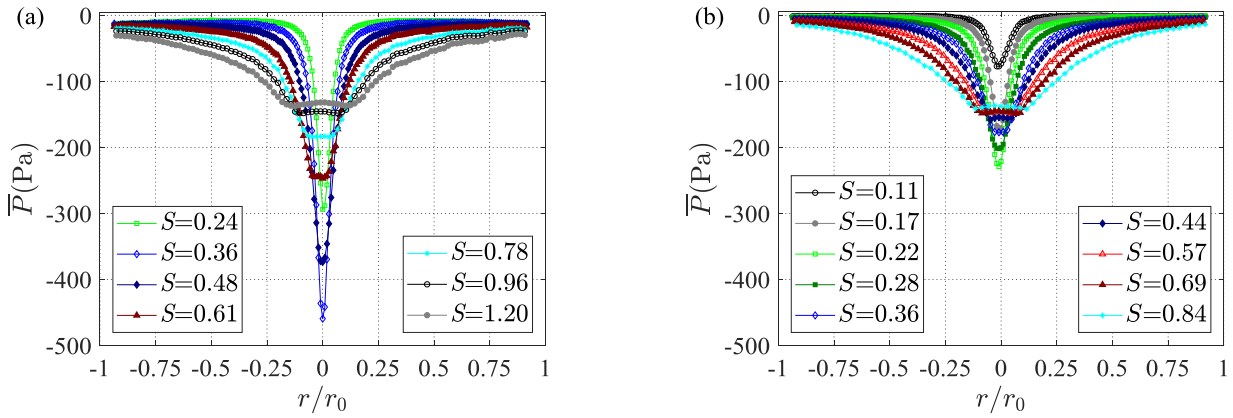

Fig. 8 Dependence of mean surface pressure deficit on swirl ratio for (a) a=0.5 and (b) a=1.0

5. Effects of the aspect ratio on the chracteristics of surface pressure deficit

The effects of the aspect ratio on the simulated vortices are also reflected in the characteristics of the mean and fluctuation components of the surface pressure deficit caused by the flow aloft.

Figs. 8(a) and 8(b), the latter of which has previously been presented in Tang *et al.* (2018), show the dependence of the radial profiles of the mean surface pressure deficit on the swirl ratio for aspect ratios of 0.5 and unity, respectively. The transition of the mean surface pressure profile due to increasing swirl ratio can be clearly observed for experiments at both aspect ratios. With increasing swirl ratio, the mean surface pressure profile transitions from one with a single valley at the center of the vortex to one with two valleys, indicating a corresponding transition of the flow aloft. The same has been shown in many previous studies (e.g., Tang *et al*. 2018, Snow *et al.* 1980, Refan and Hangan 2016). Fig. 8 also clearly shows the effect of the aspect ratio on the mean surface pressure. It is seen that at similar swirl ratios but different aspect ratios, the magnitude of the mean surface pressure deficit at the same radial positions relative to the core radius can be very different. In addition, it is of interest to notice that the flattening of the profile, which signifies the breakdown of the vortex reaching the floor, starts at a swirl ratio around 0.22 for the simulation at an aspect ratio of one, but the same starts at a swirl ratio of approximately 0.36 for the simulation at an aspect ratio of 0.5. While further investigation is needed to definitively reveal the reason behind the observed influence of the aspect ratio on the critical transition of the flow, it is speculated that the observation is related to the fact that a change of the height of the confluence region, which is the mechanism used to achieve the change in the aspect ratio, also changes the height between the simulator floor and the top of the convection zone, and that this in turn affects the downward progression of vortex break down that leads to the critical transition.

Such effects of the aspect ratio on the mean surface pressure deficit can also be clearly observed in Fig. 9(a), which shows the correlation between the maximum mean surface pressure deficit (i.e., the minimum negative pressure value at each swirl ratio) and the swirl ratio. It is seen that the maximum of the maximum mean surface pressure deficit (i.e., the minimum negative pressure value for all the swirl ratios tested), which is achieved at the critical transition of the flow from a single-celled vortex to a double-celled vortex, occurs at different swirl ratios for the simulations at the two aspect ratios. This is again evidence of the aspect ratio influencing the transition of the flow. To facilitate a further investigation of the dependence of the surface pressure deficit on the aspect ratio, a surface pressure deficit coefficient is defined as $C_P = P/(0.5\rho\bar{V}^2_{\theta\max})$, where P is the surface pressure deficit, and ρ is air density. Fig. 9(b) shows the minimum of the mean values of this coefficient against the swirl ratio for the experiments in which comprehensive velocity measurements were carried out. It is apparent that the curves based on data from the experiments at the two aspect ratios do not collapse, again indicating the effect of the aspect ratio on the simulations. Snow *et al.* (1980) proposed a form of nondimensional pressure deficit based on nondimensionalizing the tangential momentum equation and the assumption of inviscid flow with a mean tangential velocity profile of a Rankine vortex, which can be expressed as

$$C_p = \frac{P}{\frac{\rho}{2}\left(\frac{Qh}{\pi r_o^2}\right)^2 \frac{1}{a^2}} \tag{13}$$

However, we found that this form of nondimensional pressure deficit as a function of the swirl ratio does not collapse the experiemental data at the two swirl ratio either.

Fig. 10 shows the radial profiles of the mean, standard deviation, skewness and kurtosis of the surface pressure deficit coefficient for the simulations at two swirl ratios each at aspect ratios of 1 and 0.5. For simulations at both aspect ratios, the swirl ratio critically affects fluctuation characteristics, in addition to the mean characteristics, of the surface pressure. The radial profiles of the variance of the pressure fluctuation beneath the two vortices at the

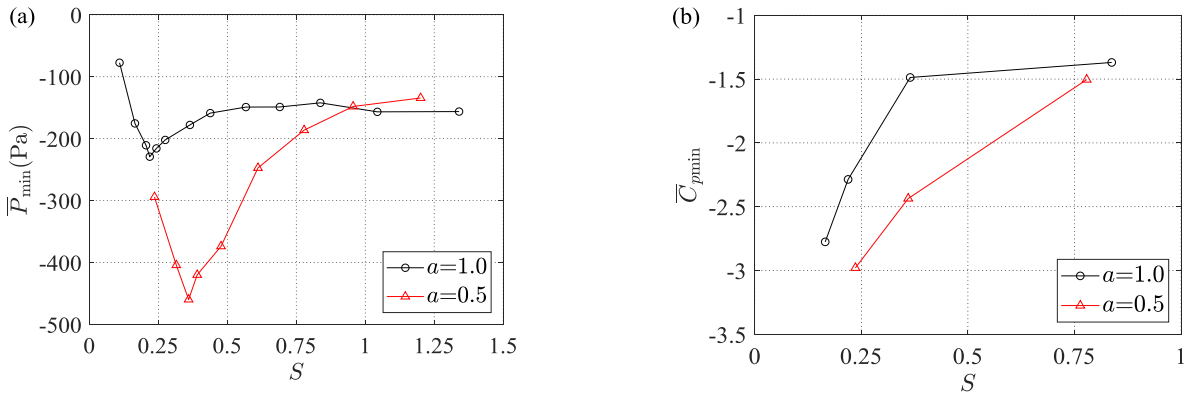

Fig. 9 Maximum mean pressure deficit versus swirl ratio: (a) dimensional pressure and (b) nondimensional pressure

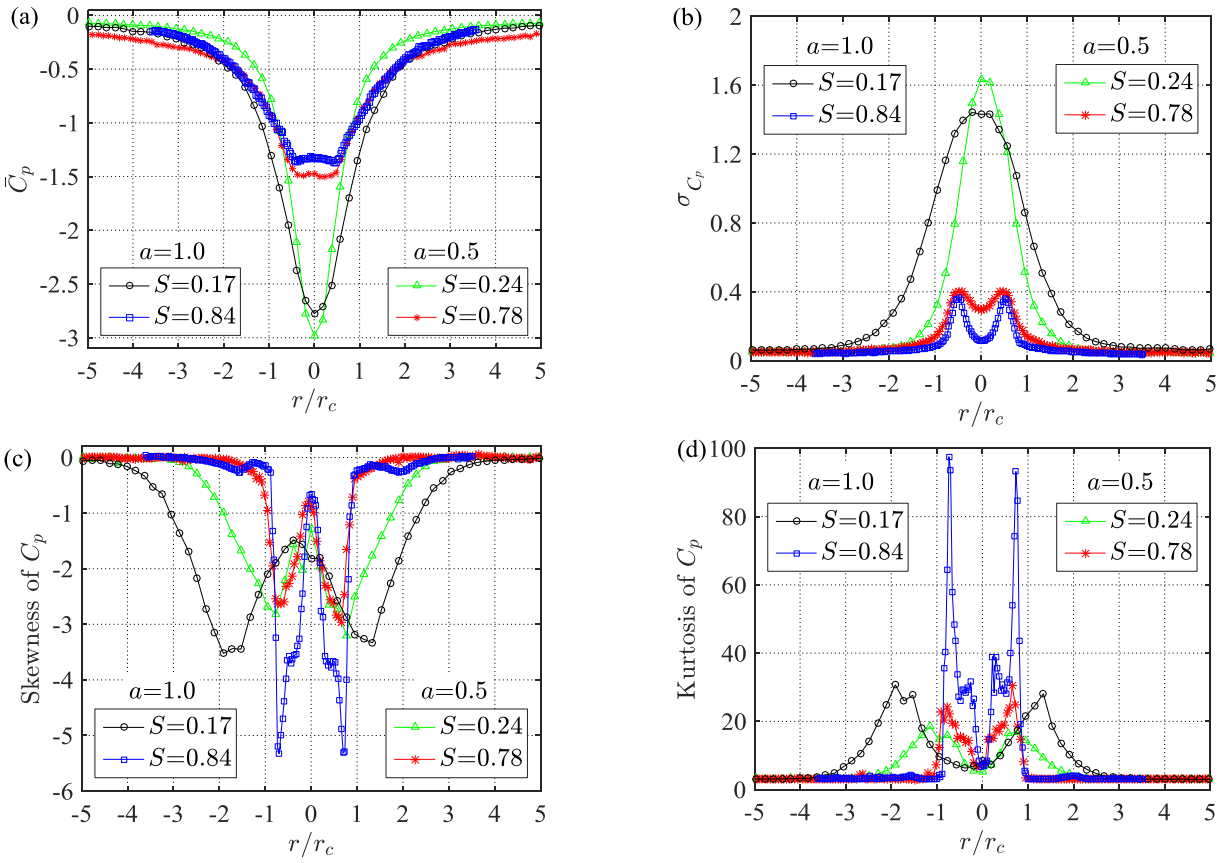

Fig. 10 Dependence of surface pressure fluctuation on swirl ratio and aspect ratio

smaller swirl ratios have a single peak, while the corresponding profiles for the two vortices at the larger swirl ratios have a bi-modal distribution. This can be attributed to the fact that as shown above, the vortices at the two smaller ratios are single-celled in structure and those at the two larger swirl ratios are two-celled in structure. In addition, the profiles of the skewness and kurtosis clearly suggest that at each aspect ratio, the surface pressure fluctuation inside and surrounding the core of the vortex is highly non-Gaussian regardless of the vortex type, and that the exact probability distribution of the pressure depends highly on the swirl ratio.

An examination of the instantaneous radial profiles of the surface pressure deficit during the simulations reveals that the significant non-Gaussian skewness (i.e., much smaller than zero) and kurtosis (i.e., much larger than 3) values are a result of intermittent occurrences of pressure deficits that are much larger than the mean values in and around the cores of the vortices. As an illustration, Fig. 11 shows two example instantaneous profiles of surface pressure deficit beneath the two vortices simulated at an aspect ratio of unity. For both cases, instantaneous large pressure deficits can be seen clearly in regions over small distances. It must be noted that while there are two such

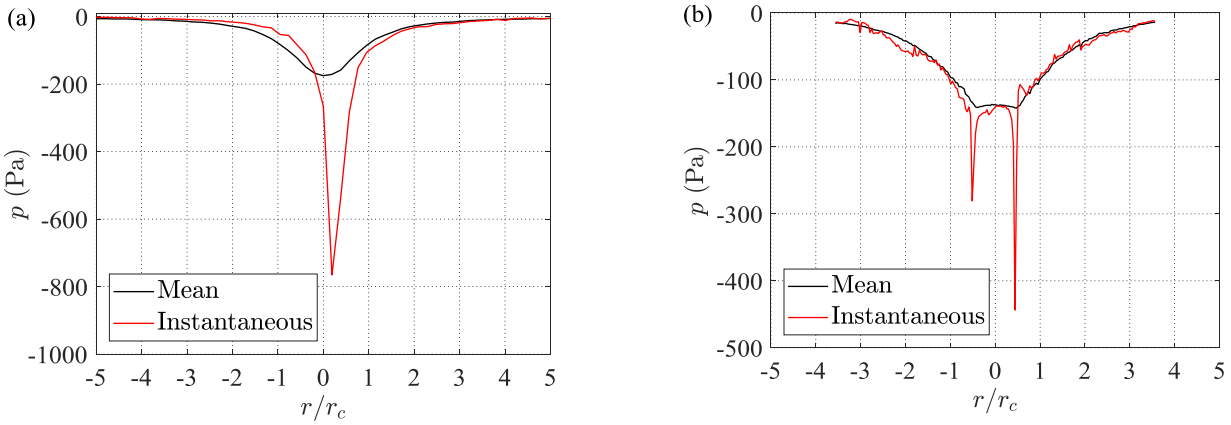

Fig. 11 Example radial profiles of instantaneous surface pressure deficit beneath vortices simulated at an aspect ratio of unity and swirl ratios of (a) S=0.17 and (b) S=0.84

regions at this particular instance, one on each side relative to the axis of the simulator, in the profile of the pressure deficit under the two-celled vortex, at some other instances, only one such region exists on one of the two sides. As it has been shown in Tang *et al.* (2018), the non-Gaussian characteristics of the pressure fluctuation are correlated with the corresponding non-Gaussian characteristics of the flow above. Although the exact cause for these non-Gaussian characteristics has not been definitively identified, an interpretation of the temporal data of the surface pressure fluctuation under the vortices reveals that the intermittent occurrences of pressure deficits that are much larger than the mean values are likely not a direct result of vortex-wandering because these occurrences can be at quite high rates (i.e., greater than 10 Hz) while vortex wandering is a low frequency phenomenon. However, it is apparent in the temporal data that vortex wandering affects the range of the region over which the intermittent large pressure deficits can occur.

Fig. 10 also suggests that the surface pressure fluctuation is significantly influenced by the aspect ratio. For vortices of the same type (i.e., single-celled or two-celled) at similar swirl ratios but different aspect ratios, while the shapes of radial profiles of the variance of the surface pressure deficit coefficient are of the same type, the magnitudes of the variance at the same radial location can be very different. The same can be concluded regarding the skewness and kurtosis of the surface pressure fluctuation. All these are an indication that the aspect ratio affects the fluctuation of the surface pressure, which further suggests that the aspect ratio affects the turbulence in the flow above the surface.

6. Conclusions

Experiments in a large-scale Ward-type simulator is used as a basis to investigate the effect of the aspect ratio on laboratory simulation of tornado-like vortices. It is found that while the swirl ratio is a major predictor of the transition of the flow from a single-celled vortex to a double-celled vortex as well as that of the mean characteristics of the flow and those of the surface pressure deficit, the aspect ratio also has secondary effects on the critical transition and the mean characteristics of the flow and pressure. In particular, besides influencing the geometry of the simulated vortex, the aspect ratio also affects the swirl ratio at which the critical transition occurs. In addition, the experiments also suggest that the aspect ratio significantly affects the characteristics of the fluctuation of the surface pressure, which is a reflection of the turbulence in the tornado-like flow aloft.

Acknowledgements

The velocity and floor pressure measurements at a simulator aspect ratio of 0.5 were conducted as a part of the Joint Research initiated in 2016 by Texas Tech University (TTU), USA and Central Research Institute of Electric Power Industry (CRIEPI), Japan. The authors at Texas Tech University acknowledge partial support from the National Science Foundation under award number CMMI 1663363. The authors also acknowledge Dr. Keisuke Nakao, CRIEPI, for his comments in discussing the measurement results.

References

Aboshosha, H., Elshaer, A., Bitsuamlak, G.T. and El Damatty, A. (2015), "Consistent inflow turbulence generator for LES evaluation of wind-induced responses for tall buildings", *J. Wind Eng. Ind. Aerod.*, **142**, 198-216.

Bryan, G.H., Dahl, N.A., Nolan, D.S. and Rotunno, R. (2017), "An eddy injection method for large-eddy simulations of tornado-like vortices", *Mon. Weather Rev.*, **145**(5), 1937-1961.

Burgers, J.M. (1948), "A Mathematical Model Illustrating the Theory of Turbulence", Advances in Applied Mechanics, (Eds., M. Richard Von, and K. Theodore Von), 171-199.

Church, C.R., Snow, J.T., Baker, G.L. and Agee, E.M. (1979), "Characteristics of tornado-like vortices as a function of swirl ratio: a laboratory investigation", *J. Atmos. Sci.*, **36**(9), 1755-1776.

Davies-Jones, R.P. (1973), "The dependence of core radius on

swirl ratio in a tornado simulator", *J. Atmos. Sci*., **30**(7), 1427-1430.
Fujita, T.T. (1971), Proposed characterization of tornadoes and hurricanes by area and intensity: Chicago.
Haan, F.L., Jr, Sarkar, P.P. and Gallus, W.A. (2008), "Design, construction and performance of a large tornado simulator for wind engineering applications", *Eng. Struct*., **30**(4), 1146-1159.
Ishihara, T., Oh, S. and Tokuyama, Y. (2011), "Numerical study on flow fields of tornado-like vortices using the LES turbulence model", *J. Wind Eng. Ind. Aerod*., **99**(4), 239-248.
Jischke, M.C. and Parang, M. (1974), "Properties of simulated tornado-like vortices", *J. Atmos. Sci.*, **31**(2), 506-512.
Karstens, C.D., Samaras, T.M., Lee, B.D., Gallus, W.A. and Finley, C.A. (2010), "Near-ground pressure and wind measurements in tornadoes", *Mon. Weather Rev*., **138**(7), 2570-2588.
Lewellen, W.S. (1962), "A solution for three-dimensional vortex flows with strong circulation", *J. Fluid Mech*., **14**(3), 420-432.
Lewellen, W.S., Lewellen, D.C. and Sykes, R.I. (1997), "Large-eddy simulation of a tornado's interaction with the surface", *J. Atmos. Sci*., **54**(5), 581-605.
Liu, K. and Pletcher, R.H. (2006), "Inflow conditions for the large eddy simulation of turbulent boundary layers: A dynamic recycling procedure", *J. Comput. Phys*., **219**(1), 1-6.
Liu, Z., Liu, H. and Cao, S. (2018), "Numerical study of the structure and dynamics of a tornado at the sub-critical vortex breakdown stage", *J. Wind Eng. Ind. Aerod*., **177**, 306-326.
Liu, Z., Zhang, C. and Ishihara, T. (2018), "Numerical study of the wind loads on a cooling tower by a stationary tornado-like vortex through LES", *J. Fluid. Struct*., **81**, 656-672.
Mehta, K.C., Minor, J.E. and McDonald, J.R. (1976), "Wind speeds analyses of April 3-4, 1974 tornadoes", *J. Struct. Div. - ASCE*, **102**(9), 1709-1724.
Nasir, Z. (2017), "Numerical modeling of tornado-like vortex and its interaction with bluff-bodies", PhD Dissertation, University of Western Ontario.
Natarajan, D. and Hangan, H. (2012), "Large eddy simulations of translation and surface roughness effects on tornado-like vortices", *J. Wind Eng. Ind. Aerod*., **104-106**, 577-584.
Nolan, D.S. and Farrell, B.F. (1999), "The structure and dynamics of tornado-like vortices", *J. Atmos. Sci*., **56**(16), 2908-2936.
Nolan, D.S., Dahl, N.A., Bryan, G.H. and Rotunno, R. (2017), "Tornado vortex structure, intensity, and surface wind gusts in large-eddy simulations with fully developed tTurbulence", *J. Atmos. Sci*., **74**(5), 1573-1597.
Refan, M. and Hangan, H. (2016), "Characterization of tornado-like flow fields in a new model scale wind testing chamber", *J. Wind Eng. Ind. Aerod*., **151**, 107-121.
Refan, M. and Hangan, H. (2018), "Near surface experimental exploration of tornado vortices", *J. Wind Eng. Ind. Aerod*., **175**, 120-135.
Rott, N. (1958), "On the viscous core of a line vortex", *Zeitschrift für angewandte Mathematik und Physik ZAMP*, **9**(5), 543-553.
Snow, J.T., Church, C.R. and Barnhart, B.J. (1980), "An investigation of the surface pressure fields beneath simulated tornado cyclones", *J. Atmos. Sci.*, **37**(5), 1013-1026.
Sullivan, R.D. (1959), "A two-cell vortex solution of the navier-stokes equations", *J. Aerosp. Sci*., **26**(11), 767-768.
Tabor, G.R. and Baba-Ahmadi, M.H. (2010), "Inlet conditions for large eddy simulation: A review", *Comput. Fluids*, **39**(4), 553-567.
Tang, Z., Feng, C., Wu, L., Zuo, D. and James, D.L. (2018), "Characteristics of tornado-like vortices simulated in a large-scale ward-type simulator", *Bound.-Lay. Meteorol*., **166**(2), 327-350.
Tang, Z., Zuo, D., James, D., Eguchi, Y. and Hattori, Y. (2018), "Effects of aspect ratio on laboratory simulation of tornado-like vortices", *Wind Struct*., Under review.
Ward, N.B. (1972), "The exploration of certain features of Tornado dynamics using a laboratory model", *J. Atmos. Sci*., **29**(6), 1194-1204.
Wurman, J. and Gill, S. (2000), "Finescale radar observations of the dimmitt, Texas (2 June 1995), tornado", *Mon. Weather Rev.*, **128**(7), 2135-2164.
Wurman, J., Kosiba, K. and Robinson, P. (2013), "In situ, doppler radar, and video observations of the interior structure of a tornado and the wind–damage relationship", *Bull. Am. Meteorol. Soc*., **94**(6), 835-846.
Wurman, J., Robinson, P., Alexander, C. and Richardson, Y. (2007), "Low-level winds in tornadoes and potential catastrophic tornado impacts in urban areas", *Bull. Am. Meteorol. Soc*., **88**(1), 31-46.
Yang, Q., Gao, R., Bai, F., Li, T. and Tamura, Y. (2018), "Damage to buildings and structures due to recent devastating wind hazards in East Asia", *Nat. Hazards*, **92**(3), 1321-1353.